

Dynamics of a subsonic rounded impinging jet

Tonal or broadband noise? Why?

Javier Sierra-Ausin^{1,2}, F. Giannetti¹, D. Fabre²

¹ UPS-IMFT, Institut de Mécanique des fluides de Toulouse, CNRS, Toulouse 31400, France

² UNISA-DIIN, Università degli Studi di Salerno, Fisciano 84084, Italy



UNIVERSITÀ
DEGLI STUDI
DI SALERNO

Table of contents

1. Motivation
2. Problem formulation
3. Linear stability
4. Wave decomposition
5. Nonlinear stability – Transition from broadband noise to tonal noise
6. Global decomposition of the flow – Non-local wavemaker identification

Motivation

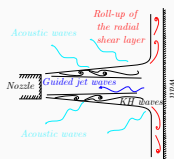
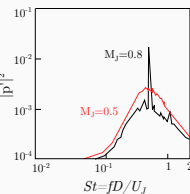
Motivation – Apparent cut-off for broadband/tonal noise

1. Experiments by Powell^a, Wagner^b, Neuwerth^c, Preisser^d and Ho & Noisseur^{e,f}, Jaunet^g (and many others) observed:

- The frequency varies with the distance to the solid boundary, and it is organised in stages.
- The dynamics of the jet, for instance pressure in the near-field and in the far-field, were found to peak at particular frequency for high subsonic Mach numbers and to be broadband for low Mach numbers.

2. Tam & Ahuja^h proposed a theoretical model for the frequency selection.

- The acoustic wave propagates inside the jet
- The feedback resonance in subsonic impinging jets must be associated with the axisymmetric mode alone whereas both helical (flapping) and axisymmetric modes are possible in supersonic jets.
- Feedback between a Kelvin-Helmholtz mode and the least dispersive acoustic guided jet wave.
- Cut-off Mach number ~ 0.6 because the $St \approx 0.7$ for the KH wave does not match the frequency of the guided waves.



^aPowell, "On edge tones and associated phenomena".

^bWagner, *The sound and flow field of an axially symmetric free jet upon impact on a wall*.

^cNeuwerth, "Acoustic feedback of a subsonic and supersonic free jet which impinges on an obstacle".

^dPreisser, *Fluctuating surface pressure and acoustic radiation for subsonic normal jet impingement*.

^eHo and Noisseur, "Dynamics of an impinging jet. Part 1. The feedback phenomenon".

^fNoisseur and Ho, "Dynamics of an impinging jet. Part 2. The noise generation".

^gJaunet et al., "Dynamics of round jet impingement".

^hTam and Ahuja, "Theoretical model of discrete tone generation by impinging jets".

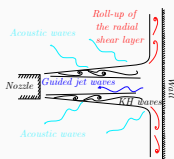
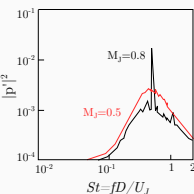
Motivation – Apparent cut-off for broadband/tonal noise

1. Experiments by Powell^a, Wagner^b, Neuwerth^c, Preisser^d and Ho & Noisseur^{e,f}, Jaunet^g (and many others) observed:

- The frequency varies with the distance to the solid boundary, and it is organised in stages. ✓ There is a feedback mechanism between a KH and an acoustic wave.
- The dynamics of the jet, for instance pressure in the near-field and in the far-field, were found to peak at particular frequency for high subsonic Mach numbers and to be broadband for low Mach numbers.

2. Tam & Ahuja^h proposed a theoretical model for the frequency selection.

- The acoustic wave propagates inside the jet
- The feedback resonance in subsonic impinging jets must be associated with the axisymmetric mode alone whereas both helical (flapping) and axisymmetric modes are possible in supersonic jets.
- Feedback between a Kelvin-Helmholtz mode and the least dispersive acoustic guided jet wave.
- Cut-off Mach number ~ 0.6 because the $St \approx 0.7$ for the KH wave does not match the frequency of the guided waves.



^aPowell, "On edge tones and associated phenomena".

^bWagner, *The sound and flow field of an axially symmetric free jet upon impact on a wall*.

^cNeuwerth, "Acoustic feedback of a subsonic and supersonic free jet which impinges on an obstacle".

^dPreisser, *Fluctuating surface pressure and acoustic radiation for subsonic normal jet impingement*.

^eHo and Noisseur, "Dynamics of an impinging jet. Part 1. The feedback phenomenon".

^fNoisseur and Ho, "Dynamics of an impinging jet. Part 2. The noise generation".

^gJaunet et al., "Dynamics of round jet impingement".

^hTam and Ahuja, "Theoretical model of discrete tone generation by impinging jets".

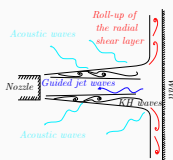
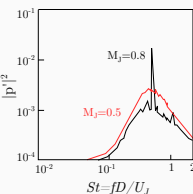
Motivation – Apparent cut-off for broadband/tonal noise

1. Experiments by Powell^a, Wagner^b, Neuwerth^c, Preisser^d and Ho & Nossir^{e,f}, Jaunet^g (and many others) observed:

- The frequency varies with the distance to the solid boundary, and it is organised in stages. ✓ There is a feedback mechanism between a KH and an acoustic wave.
- The dynamics of the jet, for instance pressure in the near-field and in the far-field, were found to peak at particular frequency for high subsonic Mach numbers and to be broadband for low Mach numbers.

2. Tam & Ahuja^h proposed a theoretical model for the frequency selection.

- The acoustic wave propagates inside the jet ✓ Guided (m, n) jet modes. m -azimuthal number and n radial number.
- The feedback resonance in subsonic impinging jets must be associated with the axisymmetric mode alone whereas both helical (flapping) and axisymmetric modes are possible in supersonic jets.
- Feedback between a Kelvin-Helmholtz mode and the least dispersive acoustic guided jet wave.
- Cut-off Mach number ~ 0.6 because the $St \approx 0.7$ for the KH wave does not match the frequency of the guided waves.



^aPowell, "On edge tones and associated phenomena".

^bWagner, *The sound and flow field of an axially symmetric free jet upon impact on a wall*.

^cNeuwerth, "Acoustic feedback of a subsonic and supersonic free jet which impinges on an obstacle".

^dPreisser, *Fluctuating surface pressure and acoustic radiation for subsonic normal jet impingement*.

^eHo and Nossir, "Dynamics of an impinging jet. Part 1. The feedback phenomenon".

^fNossir and Ho, "Dynamics of an impinging jet. Part 2. The noise generation".

^gJaunet et al., "Dynamics of round jet impingement".

^hTam and Ahuja, "Theoretical model of discrete tone generation by impinging jets".

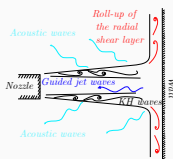
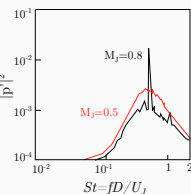
Motivation – Apparent cut-off for broadband/tonal noise

1. Experiments by Powell^a, Wagner^b, Neuwerth^c, Preisser^d and Ho & Nossir^{e,f}, Jaunet^g (and many others) observed:

- The frequency varies with the distance to the solid boundary, and it is organised in stages. ✓ There is a feedback mechanism between a KH and an acoustic wave.
- The dynamics of the jet, for instance pressure in the near-field and in the far-field, were found to peak at particular frequency for high subsonic Mach numbers and to be broadband for low Mach numbers.

2. Tam & Ahuja^h proposed a theoretical model for the frequency selection.

- The acoustic wave propagates inside the jet ✓ Guided (m, n) jet modes. m -azimuthal number and n radial number.
- The feedback resonance in subsonic impinging jets must be associated with the axisymmetric mode alone whereas both helical (flapping) and axisymmetric modes are possible in supersonic jets. ✓ Guided jet mode (0, 1) for subsonic jets and both (0, 1) and (1, 1) for supersonic jets.
- Feedback between a Kelvin-Helmholtz mode and the least dispersive acoustic guided jet wave. ✗ The derivative of the group velocity with respect to the wavenumber is small.
- Cut-off Mach number ~ 0.6 because the $St \approx 0.7$ for the KH wave does not match the frequency of the guided waves.



^aPowell, "On edge tones and associated phenomena".

^bWagner, *The sound and flow field of an axially symmetric free jet upon impact on a wall*.

^cNeuwerth, "Acoustic feedback of a subsonic and supersonic free jet which impinges on an obstacle".

^dPreisser, *Fluctuating surface pressure and acoustic radiation for subsonic normal jet impingement*.

^eHo and Nossir, "Dynamics of an impinging jet. Part 1. The feedback phenomenon".

^fNossir and Ho, "Dynamics of an impinging jet. Part 2. The noise generation".

^gJaunet et al., "Dynamics of round jet impingement".

^hTam and Ahuja, "Theoretical model of discrete tone generation by impinging jets".

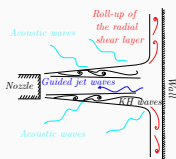
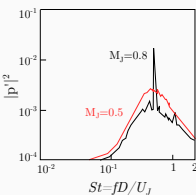
Motivation – Apparent cut-off for broadband/tonal noise

1. Experiments by Powell^a, Wagner^b, Neuwerth^c, Preisser^d and Ho & Nossir^{e,f}, Jaunet^g (and many others) observed:

- The frequency varies with the distance to the solid boundary, and it is organised in stages. ✓ There is a feedback mechanism between a KH and an acoustic wave.
- The dynamics of the jet, for instance pressure in the near-field and in the far-field, were found to peak at particular frequency for high subsonic Mach numbers and to be broadband for low Mach numbers.

2. Tam & Ahuja^h proposed a theoretical model for the frequency selection.

- The acoustic wave propagates inside the jet ✓ Guided (m, n) jet modes. m -azimuthal number and n radial number.
- The feedback resonance in subsonic impinging jets must be associated with the axisymmetric mode alone whereas both helical (flapping) and axisymmetric modes are possible in supersonic jets. ✓ Guided jet mode (0, 1) for subsonic jets and both (0, 1) and (1, 1) for supersonic jets.
- Feedback between a Kelvin-Helmholtz mode and the least dispersive acoustic guided jet wave. ✗ The derivative of the group velocity with respect to the wavenumber is small.
- Cut-off Mach number ~ 0.6 because the $St \approx 0.7$ for the KH wave does not match the frequency of the guided waves. ✗ There is a global mode for every Mach number. We need nonlinear theory.



^aPowell, "On edge tones and associated phenomena".

^bWagner, *The sound and flow field of an axially symmetric free jet upon impact on a wall*.

^cNeuwerth, "Acoustic feedback of a subsonic and supersonic free jet which impinges on an obstacle".

^dPreisser, *Fluctuating surface pressure and acoustic radiation for subsonic normal jet impingement*.

^eHo and Nossir, "Dynamics of an impinging jet. Part 1. The feedback phenomenon".

^fNossir and Ho, "Dynamics of an impinging jet. Part 2. The noise generation".

^gJaunet et al., "Dynamics of round jet impingement".

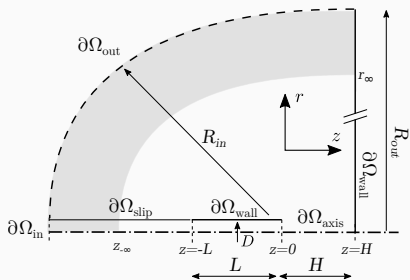
^hTam and Ahuja, "Theoretical model of discrete tone generation by impinging jets".

Formulation

Governing equations

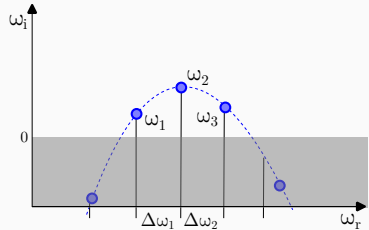
$$\mathbf{B} \frac{\partial \mathbf{q}}{\partial t} = \mathbf{F}(\mathbf{q}, \eta) \quad \text{with } \mathbf{B} = \text{diag}(1, \rho \mathbf{I}, \rho, 0), \quad (1)$$

$$\mathbf{F}(\mathbf{q}, \eta) = - \begin{pmatrix} \mathbf{u} \cdot \nabla \rho + \rho \nabla \cdot \mathbf{u} \\ \rho \mathbf{u} \cdot \nabla \mathbf{u} - \nabla p + \nabla \cdot \tau(\mathbf{u}) \\ (\gamma - 1) [\rho T \nabla \cdot \mathbf{u} - \gamma M_\infty^2 \tau(\mathbf{u}) : \mathbf{D}(\mathbf{u})] + \rho \mathbf{u} \cdot \nabla T + \frac{\gamma}{\Pr \Re} \nabla^2 T \\ -\rho T + 1 + \gamma M_\infty^2 p \end{pmatrix}, \quad (2)$$



Linear Stability

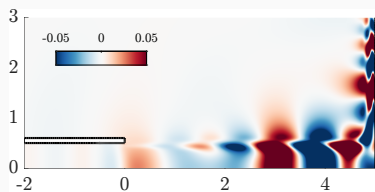
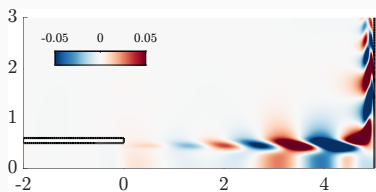
Linear stability (I)



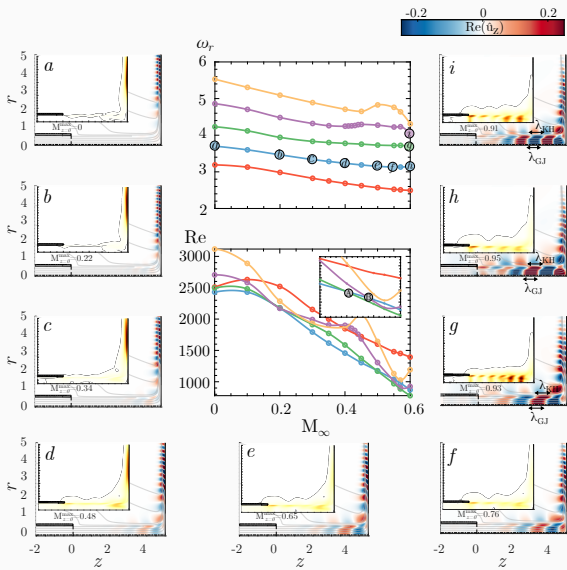
1. Linear eigenvalue problem for the global modes^a

$$-i\omega \mathbf{B}|_{q_0} \hat{\mathbf{q}} + \mathbf{D}\mathbf{F}|_{q_0}(\hat{\mathbf{q}}) = 0, \quad (3)$$

^aSierra, Fabre, and Citro, "Efficient stability analysis of fluid flows using complex mapping techniques".



Linear stability (II)



Wave decomposition

Wave decomposition of the main feedback (I)

We perform the weakly non-parallel expansion

$$\mathbf{q}(r, z) = [\mathbf{u}, p, T, \rho]^T(r, z) = \epsilon^n e^{\frac{i}{\epsilon} \int \alpha(z) dz} \sum \tilde{\mathbf{q}}_n(r)$$

Wave decomposition of the main feedback (I)

We perform the weakly non-parallel expansion

$$\mathbf{q}(r, z) = [\mathbf{u}, p, T, \rho]^T(r, z) = \epsilon^n e^{\frac{i}{\epsilon} \int \alpha(z) dz} \sum \tilde{\mathbf{q}}_n(r)$$

Determined from a multiple scales analysis

$O(0)$	$(-i\omega \mathbf{B} + D\mathbf{F}(\alpha))\tilde{\mathbf{q}}_0$	Eig. problem for α
$O(\epsilon)$	$(-i\omega \mathbf{B} + D\mathbf{F}(\alpha))\tilde{\mathbf{q}}_1 = i \frac{d}{d\alpha} (-i\omega \mathbf{B} + D\mathbf{F}(\alpha)) \frac{\tilde{\mathbf{q}}_0}{dz}$	Forced problem

(4)

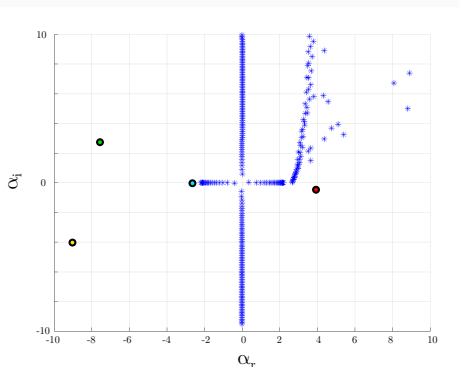
Wave decomposition of the main feedback (I)

We perform the weakly non-parallel expansion

$$\mathbf{q}(r, z) = [\mathbf{u}, p, T, \rho]^T(r, z) = \epsilon^n e^{\frac{i}{\epsilon} \int \alpha(z) dz} \sum \tilde{\mathbf{q}}_n(r)$$

Determined from a multiple scales analysis

$$\begin{aligned} O(0) \quad & (-i\omega \mathbf{B} + D\mathbf{F}(\alpha))\tilde{\mathbf{q}}_0 && \text{Eig. problem for } \alpha \\ O(\epsilon) \quad & (-i\omega \mathbf{B} + D\mathbf{F}(\alpha))\tilde{\mathbf{q}}_1 = i \frac{d}{d\alpha} (-i\omega \mathbf{B} + D\mathbf{F}(\alpha)) \frac{\tilde{\mathbf{q}}_0}{dz} && \text{Forced problem} \end{aligned} \quad (4)$$



Wave decomposition of the main feedback (I)

We perform the weakly non-parallel expansion

$$\mathbf{q}(r, z) = [\mathbf{u}, p, T, \rho]^T(r, z) = \epsilon^n e^{\frac{i}{\epsilon} \int \alpha(z) dz} \sum \tilde{\mathbf{q}}_n(r)$$

Determined from a multiple scales analysis

$$\begin{aligned} O(0) \quad & (-i\omega \mathbf{B} + D\mathbf{F}(\alpha))\tilde{\mathbf{q}}_0 && \text{Eig. problem for } \alpha \\ O(\epsilon) \quad & (-i\omega \mathbf{B} + D\mathbf{F}(\alpha))\tilde{\mathbf{q}}_1 = i \frac{d}{d\alpha} (-i\omega \mathbf{B} + D\mathbf{F}(\alpha)) \frac{\tilde{\mathbf{q}}_0}{dz} && \text{Forced problem} \end{aligned} \quad (4)$$

After imposing solvability condition

$$\mathbf{q}(z) = C_0 e^{i \int \alpha + \delta \alpha dz} \tilde{\mathbf{q}}_0 \text{ where } \delta \alpha = \frac{\tilde{\mathbf{q}}_0^\dagger \cdot \left[\frac{d}{d\alpha} (-i\omega \mathbf{B} + D\mathbf{F}(\alpha)) \frac{\tilde{\mathbf{q}}_0}{dz} \right]}{\tilde{\mathbf{q}}_0^\dagger \cdot \left[\frac{d}{d\alpha} (-i\omega \mathbf{B} + D\mathbf{F}(\alpha)) \tilde{\mathbf{q}}_0 \right]}$$

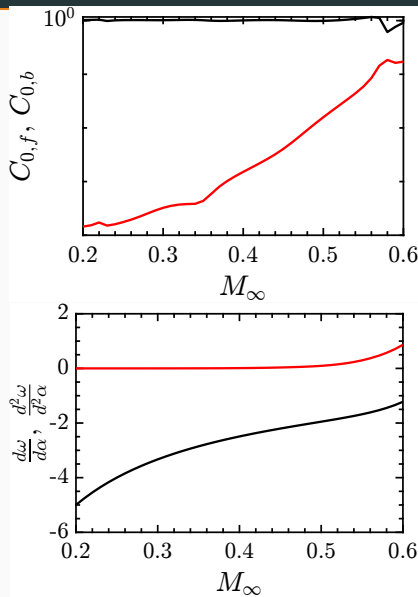
Then we can expand the linear global mode in a weakly non-parallel basis

$$\hat{\mathbf{q}} \approx \sum_k C_{0,k} e^{i \int \alpha_k + \delta \alpha_k dz} \tilde{\mathbf{q}}_{0,k}$$

then finally,

$$C_{0,k} \approx \tilde{\mathbf{q}}_0^\dagger \cdot \left[\frac{d}{d\alpha} (-i\omega \mathbf{B} + D\mathbf{F}(\alpha)) \hat{\mathbf{q}} \right] e^{-i \int \alpha_k + \delta \alpha_k dz}$$

Wave decomposition of the main feedback (II)

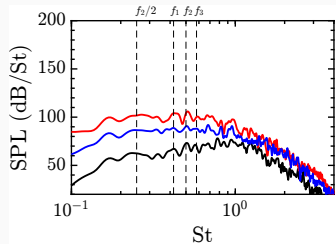


1. Projection of local modes on the global mode for $St \approx 0.5$, as a function of the Mach number at the critical Reynolds number.
 - Projection of the guided acoustic wave (red) and the KH mode (black)
 - The projection of the remaining terms is negligible
2. Tam & Ahuja (1990)^a suggestion
 - For a turbulent jet, the frequency selection is dictated only by the acoustic backward wave which is the least dispersive, i.e. $Re(\frac{d^2\omega}{d\alpha^2}) = 0$
 - Using this reasoning, the discrete tone generation is not possible for $M_J < 0.6$. The frequency of the acoustic guided jet wave lies outside the frequency range of KH instabilities.

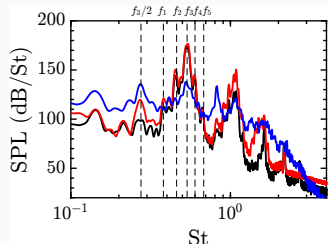
Nonlinear stability – Transition from broadband noise to tonal noise

Axisymmetric DNS

$M_J \approx 0.35$, $\text{Re} = 2000$



$M_J \approx 0.9$, $\text{Re} = 2000$

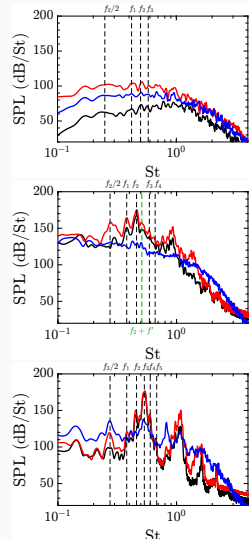


Normal form - Main feedback (I)

Consider the parametrization of dynamics

$$\mathbf{q} = \mathbf{q}_0 + \sum_j [r_j e^{i\phi_j(t)} \hat{\mathbf{q}} + \text{c.c.}] + \text{higher harmonics}$$
$$\dot{r}_j = r_j (\lambda_j + \sum_k^N \nu_{jk} r_k^2) + r_{j+1} r_{j-1} \cos(\psi_j) \text{Re}(\chi_j) + r_{j+1} r_j r_{j-1} \sin(\psi_j) \text{Im}(\chi_j)$$
$$\dot{\psi}_j = \delta\omega + F_{\psi_j}(\mathbf{r}, \Psi).$$

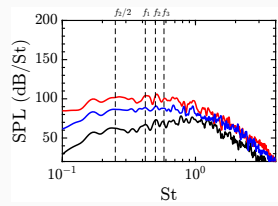
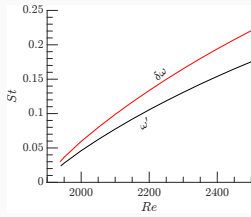
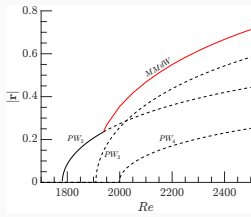
- Three main cases:
 - (a) Tonal resonance:
 - Monochromatic dynamics: Strict monochromatic dynamics only near transition. Larger interval for large subsonic Mach numbers.
 - Quasi-periodic resonance: Two incommensurate frequencies lead to the excitation of every (unstable) global mode, which are phase-locked.
 - (b) Hopf bifurcation of the case (a.ii): Slow desynchronization of the quasi-periodic attractor with a slow frequency $f' \propto \delta\omega$, it occurs for $0.4 < M_J < 0.7$
 - (c) Route towards chaos/broadband spectrum when $f' \approx \Delta\omega$, it occurs for $M_J < 0.4$



Normal form - Main feedback (II)

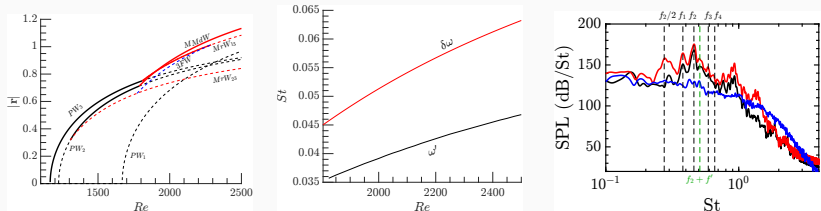
At low subsonic Mach number, we consider $M_J \approx 0.35$,

$$\begin{aligned}
 \dot{r}_1 &= r_1 (\lambda_1 + \nu_{11} r_1^2 + \nu_{12} r_2^2 + \nu_{13} r_3^2) \\
 &\quad + r_2^2 r_3 (\cos(\psi_j) \operatorname{Re}(\chi_1)) + \sin(\psi) \operatorname{Im}(\chi_1)) \\
 \dot{r}_2 &= r_2 (\lambda_2 + \nu_{21} r_1^2 + \nu_{22} r_2^2 + \nu_{23} r_3^2) \\
 &\quad + r_1 r_2 r_3 (\cos(\psi) \operatorname{Re}(\chi_2)) + \sin(\psi) \operatorname{Im}(\chi_2)) \\
 \dot{r}_3 &= r_3 (\lambda_3 + \nu_{31} r_1^2 + \nu_{32} r_2^2 + \nu_{33} r_3^2) \\
 &\quad + r_2^2 r_1 (\cos(\psi_j) \operatorname{Re}(\chi_1)) + \sin(\psi) \operatorname{Im}(\chi_1)) \\
 \dot{\psi}_j &= [\delta\omega] + \\
 &\quad \cos(\psi) [\operatorname{Im}(\chi_3) r_1 r_2^2 / r_3 + 2\operatorname{Im}(\chi_2) r_1 r_3 - \operatorname{Im}(\chi_1) r_3 r_2^2 / r_1] \\
 &\quad - \sin(\psi) [\operatorname{Re}(\chi_3) r_1 r_2^2 / r_3 + \operatorname{Re}(\chi_2) r_1 r_3 + \operatorname{Re}(\chi_1) r_2^2 r_3 / r_1].
 \end{aligned}$$

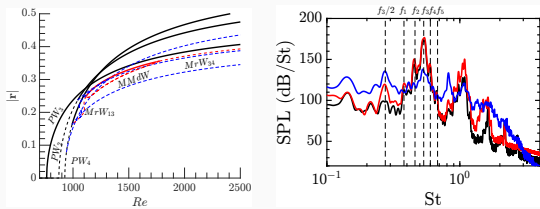


Normal form - Main feedback (III)

At intermediate subsonic Mach number, we consider $M_J \approx 0.65$,



At high subsonic Mach number, we consider $M_J \approx 0.9$,



Global decomposition of the flow – Non-local wavemaker identification

Decomposition of the global modes (I)

The linear perturbation $\hat{\mathbf{q}}$ is herein decomposed into three components: *acoustic*, *hydrodynamic* and *entropic*¹²,

For this purpose, we adopt a Helmholtz-Hodge decomposition³ of the perturbation velocity field into *acoustic* (potential) and *hydrodynamic* (solenoidal)

$$\hat{\mathbf{u}} = \hat{\mathbf{u}}_{ac} + \hat{\mathbf{u}}_{hyd} = \nabla\phi_c + \nabla \times \Psi \quad (5)$$

applying the divergence operator, the potential ϕ_c is determined from the following Poisson equation

$$\begin{aligned}\Delta\phi_c &= \nabla \cdot \hat{\mathbf{u}} && \text{in } \Omega \\ \nabla\phi_c \cdot \mathbf{n} &= \hat{\mathbf{u}} \cdot \mathbf{n} && \text{on } \partial\Omega.\end{aligned}$$

The hydrodynamic component of the velocity is subsequently determined by subtracting $\hat{\mathbf{u}}_{hyd} = \hat{\mathbf{u}} - \hat{\mathbf{u}}_{ac} = \hat{\mathbf{u}} - \nabla\phi_c$.

¹Ewert and Schröder, "Acoustic perturbation equations based on flow decomposition via source filtering".

²Spieser, "Modélisation de la propagation du bruit de jet par une méthode adjointe formulée pour l'acoustique potentielle".

³Schoder, Roppert, and Kaltenbacher, "Helmholtz's decomposition for compressible flows and its application to computational aeroacoustics".

Decomposition of the global modes (II)

The pressure decomposition is derived from the linearised momentum equation. Considering an isenstropic relationship between density and pressure fluctuations, i.e. $\hat{\rho}T_0 = M_\infty^2 \hat{p}$, and taking divergence of the linearised momentum equation, we end up with the following elliptic equation for the pressure,

$$-\Delta \frac{\hat{p}}{\rho_0} - \frac{M_\infty^2}{T_0} (\mathbf{u}_0 \cdot \nabla \mathbf{u}_0) \frac{\hat{p}}{\rho_0} = i\omega \nabla \cdot \hat{\mathbf{u}} + \nabla \cdot (\mathbf{u}_0 \cdot \nabla \hat{\mathbf{u}}) + \nabla \cdot (\hat{\mathbf{u}} \cdot \nabla \mathbf{u}_0) - \frac{1}{Re} \nabla \cdot (\nabla \cdot \tau(\hat{\mathbf{u}})). \quad (6)$$

Decomposing the velocity field into acoustic and hydrodynamic and leaving the viscous dissipation term to the entropic component, we end up with the following decomposition of the pressure,

$$\begin{aligned} -\Delta \frac{\hat{p}_{ac}}{\rho_0} - \frac{M_\infty^2}{T_0} (\mathbf{u}_0 \cdot \nabla \mathbf{u}_0) \frac{\hat{p}_{ac}}{\rho_0} &= i\omega \nabla \cdot \hat{\mathbf{u}}_{ac} + \nabla \cdot (\mathbf{u}_0 \cdot \nabla \hat{\mathbf{u}}_{ac}) + \nabla \cdot (\hat{\mathbf{u}}_{ac} \cdot \nabla \mathbf{u}_0) \\ -\Delta \frac{\hat{p}_{hyd}}{\rho_0} - \frac{M_\infty^2}{T_0} (\mathbf{u}_0 \cdot \nabla \mathbf{u}_0) \frac{\hat{p}_{hyd}}{\rho_0} &= \nabla \cdot (\mathbf{u}_0 \cdot \nabla \hat{\mathbf{u}}_{hyd}) + \nabla \cdot (\hat{\mathbf{u}}_{hyd} \cdot \nabla \mathbf{u}_0) \\ -\Delta \frac{\hat{p}_s}{\rho_0} - \frac{M_\infty^2}{T_0} (\mathbf{u}_0 \cdot \nabla \mathbf{u}_0) \frac{\hat{p}_s}{\rho_0} &= -\frac{1}{Re} \nabla \cdot (\nabla \cdot \tau(\hat{\mathbf{u}})). \end{aligned}$$

Decomposition of the global modes (III)

Density and temperature are recovered from the pressure,

$$\hat{T}_{\text{ac}} = (\gamma - 1) M_{\infty}^2 \hat{\rho}_{\text{ac}}, \quad \hat{T}_{\text{hyd}} = (\gamma - 1) M_{\infty}^2 \hat{\rho}_{\text{hyd}}, \quad \hat{T}_s = \hat{T} - \hat{T}_{\text{ac}} - \hat{T}_{\text{hyd}}, \quad (7)$$

$$\hat{\rho}_{\text{ac}} = M_{\infty}^2 \frac{\rho_0}{T_0} \hat{\rho}_{\text{ac}}, \quad \hat{\rho}_{\text{hyd}} = M_{\infty}^2 \frac{\rho_0}{T_0} \hat{\rho}_{\text{hyd}}, \quad \hat{\rho}_s = \hat{\rho} - \hat{\rho}_{\text{ac}} - \hat{\rho}_{\text{hyd}}. \quad (8)$$

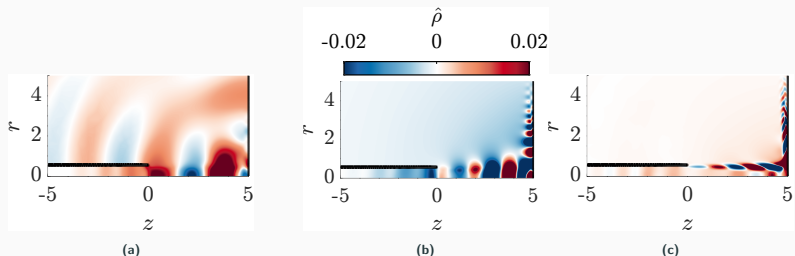


Figure 1: Density decomposition of the global mode with $St \approx 0.5$ at criticality ($Re = 900$) at $M_{\infty} = 0.6$ ($M_J \approx 0.9$). (a) Acoustic component of density $\hat{\rho}_{\text{ac}}$. (b) Hydrodynamic component of density $\hat{\rho}_{\text{hyd}}$. (c) Entropic component of density $\hat{\rho}_s$

Decomposition of the global modes (IV)

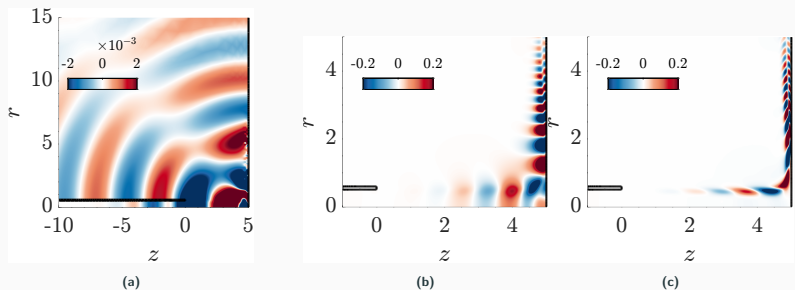


Figure 2: Density decomposition of the global mode with $St \approx 0.5$ at criticality ($Re \approx 1500$) at $M_\infty = 0.4$ ($M_J \approx 0.45$). (a) Acoustic component of density $\hat{\rho}_{\text{ac}}$. (b) Hydrodynamic component of density $\hat{\rho}_{\text{hyd}}$. (c) Entropic component of density $\hat{\rho}_s$

Non-local structural sensitivity decomposition

What happens if we introduce a small spatially localised linear harmonic feedback term $\mathbf{H}(\hat{\mathbf{q}}) \equiv \delta(\mathbf{x} - \mathbf{x}_0)\mathbf{P}_H\mathbf{C}_0\mathbf{P}_{\hat{\mathbf{q}}}\hat{\mathbf{q}}$?

$$\left(-i\omega\mathbf{B}|_{\mathbf{q}_0} + \mathbf{D}\mathbf{F}|_{\mathbf{q}_0} \right) \hat{\mathbf{q}} = \mathbf{H}(\hat{\mathbf{q}}). \quad (9)$$

\mathbf{P}_H a diagonal matrix that selects the type of forcing. In the following, we neglect mass injection to the system, and we simply consider momentum forcing and a source of heat release, that is, $\mathbf{P}_H = \text{diag}(0, \mathbf{I}, 1, 0, 0)$.

$$i\delta\omega = \langle \mathbf{P}_H\hat{\mathbf{q}}^\dagger, \delta(\mathbf{x} - \mathbf{x}_0)\mathbf{C}_0\mathbf{P}_{\hat{\mathbf{q}}}\hat{\mathbf{q}} \rangle \leq \|\mathbf{C}_0\| \|\mathbf{P}_H\hat{\mathbf{q}}^\dagger\|_{L^2} \|\mathbf{P}_{\hat{\mathbf{q}}}\hat{\mathbf{q}}\|_{L^2} = \|\mathbf{C}_0\| \mathbf{S}_s(\mathbf{x}_0), \quad (10)$$

that is, the structural sensitivity map is defined as $\mathbf{S}_s(\mathbf{x}_0) \equiv \|\mathbf{P}_H\hat{\mathbf{q}}^\dagger\|_{L^2} \|\mathbf{P}_{\hat{\mathbf{q}}}\hat{\mathbf{q}}\|_{L^2}$. The scalar field \mathbf{S}_s is then an upper bound function for the eigenvalue variation that can be employed to determine locations where the feedback is stronger, identifying in this way the regions where the instability mechanism act.

However, when it is not localized within a small physical region, it does not clearly identify the *wavemaker*, but a possible interacting region between the components of the global mode.

A two-step decomposition of the forcing term (I)

Decomposing the mode $\hat{\mathbf{q}}$ we can rewrite the harmonic forcing as

$\mathbf{H}(\hat{\mathbf{q}}) = \mathbf{H}(\hat{\mathbf{q}}_{\text{ac}} + \hat{\mathbf{q}}_{\text{hyd}} + \hat{\mathbf{q}}_{\text{s}})$, which due to linearity of the forcing term on the eigenmode is simply expressed as

$$\mathbf{H}(\hat{\mathbf{q}}) = \mathbf{H}(\hat{\mathbf{q}}_{\text{ac}}) + \mathbf{H}(\hat{\mathbf{q}}_{\text{hyd}}) + \mathbf{H}(\hat{\mathbf{q}}_{\text{s}}). \quad (11)$$

Thus, we have a first decomposition of the harmonic forcing $\mathbf{H}(\hat{\mathbf{q}})$ from the splitting of the state variable. However, the term $\mathbf{H}(\hat{\mathbf{q}}_{\text{ac}})$ is not necessarily a forcing term that uniquely induces acoustic perturbations. Assume, for simplicity, that the previous forcing term depends uniquely on the acoustic velocity, $\mathbf{H}(\mathbf{u}_{\text{ac}})$, and it only acts on the momentum equation, that is, we neglect mass or heat injection.

$$\begin{aligned} & \frac{\partial \hat{\omega}}{\partial t} + \mathbf{u}_0 \cdot \nabla \hat{\omega} + \hat{\mathbf{u}} \cdot \nabla \omega_0 + \omega_0 (\nabla \cdot \hat{\mathbf{u}}) + \hat{\omega} (\nabla \cdot \mathbf{u}_0) - \\ & \frac{1}{\rho_0^2} \nabla p_0 \times \nabla \hat{p} + \frac{1}{\rho_0^2} \nabla \hat{p} \times \nabla p_0 - \nabla \times (\tau(\hat{\mathbf{u}})/\rho_0) = \nabla \times \mathbf{H}_u(\mathbf{u}) \end{aligned}$$

The forcing term must be rotational-free, i.e., $\nabla \times \mathbf{H}(\mathbf{u}_{\text{ac}}) = 0$, otherwise it will induce vortical perturbations into the flow. Therefore, $\mathbf{H}(\hat{\mathbf{q}}_{\text{ac}})$ should be interpreted as a generic forcing term that depends on the acoustic perturbation.

A two-step decomposition of the forcing term (II)

To determine the effect of the forcing, that is, which kind of response induces, we decompose the forcing operator into $\mathbf{H} = \mathbf{H}_{ac} + \mathbf{H}_{hyd} + \mathbf{H}_s$. When the forcing term does not inject mass into the system, the adjoint-mode decomposition is bi-orthogonal, then the adjoint can be used to project the forcing term.

That is, $\mathbf{H}_{ac}(\hat{\mathbf{q}}) = \langle \hat{\mathbf{q}}_{ac}^\dagger, \mathbf{H}(\hat{\mathbf{q}}) \rangle \hat{\mathbf{q}}_{ac}$, $\mathbf{H}_{hyd}(\hat{\mathbf{q}}) = \langle \hat{\mathbf{q}}_{hyd}^\dagger, \mathbf{H}(\hat{\mathbf{q}}) \rangle \hat{\mathbf{q}}_{hyd}$ and

$\mathbf{H}_s(\hat{\mathbf{q}}) = \langle \hat{\mathbf{q}}_s^\dagger, \mathbf{H}(\hat{\mathbf{q}}) \rangle \hat{\mathbf{q}}_s$. With the following decomposition of the linearized problem,

$$\begin{cases} -i\omega \mathbf{B}|_{\mathbf{q}_0} + \mathbf{DF}|_{\mathbf{q}_0} + \langle \hat{\mathbf{q}}_{ac}^\dagger, \mathbf{H}(\hat{\mathbf{q}}_{ac}) \rangle + \langle \hat{\mathbf{q}}_{ac}^\dagger, \mathbf{H}(\hat{\mathbf{q}}_{hyd}) \rangle + \langle \hat{\mathbf{q}}_{ac}^\dagger, \mathbf{H}(\hat{\mathbf{q}}_s) \rangle \Big) \hat{\mathbf{q}}_{ac} = 0 \\ -i\omega \mathbf{B}|_{\mathbf{q}_0} + \mathbf{DF}|_{\mathbf{q}_0} + \langle \hat{\mathbf{q}}_{hyd}^\dagger, \mathbf{H}(\hat{\mathbf{q}}_{ac}) \rangle + \langle \hat{\mathbf{q}}_{hyd}^\dagger, \mathbf{H}(\hat{\mathbf{q}}_{hyd}) \rangle + \langle \hat{\mathbf{q}}_{hyd}^\dagger, \mathbf{H}(\hat{\mathbf{q}}_s) \rangle \Big) \hat{\mathbf{q}}_{hyd} = 0 \\ -i\omega \mathbf{B}|_{\mathbf{q}_0} + \mathbf{DF}|_{\mathbf{q}_0} + \langle \hat{\mathbf{q}}_s^\dagger, \mathbf{H}(\hat{\mathbf{q}}_{ac}) \rangle + \langle \hat{\mathbf{q}}_s^\dagger, \mathbf{H}(\hat{\mathbf{q}}_{hyd}) \rangle + \langle \hat{\mathbf{q}}_s^\dagger, \mathbf{H}(\hat{\mathbf{q}}_s) \rangle \Big) \hat{\mathbf{q}}_s = 0, \end{cases}$$

An inspection the previous equation suggests the definition of a *non-local structural sensitivity* matrix as

$$\begin{aligned} i\delta\omega_j^k &= \langle \hat{\mathbf{q}}_k^\dagger, \delta(\mathbf{x} - \mathbf{x}_0) \mathbf{C}_0 \hat{\mathbf{q}}_j \rangle \leq \|\mathbf{C}_0\| \|\hat{\mathbf{q}}_k^\dagger(\mathbf{x}_0)\| \|\hat{\mathbf{q}}_j(\mathbf{x}_0)\| = \|\mathbf{C}_0\| \mathbf{S}^{(j,k)}_s(\mathbf{x}_0), \\ \mathbf{S}^{(j,k)}_s(\mathbf{x}_0) &= \|\hat{\mathbf{q}}_k^\dagger(\mathbf{x}_0)\| \|\hat{\mathbf{q}}_j(\mathbf{x}_0)\| \text{ with } j, k = ac, hyd, s. \end{aligned}$$

Non-local structural sensitivity decomposition (II)

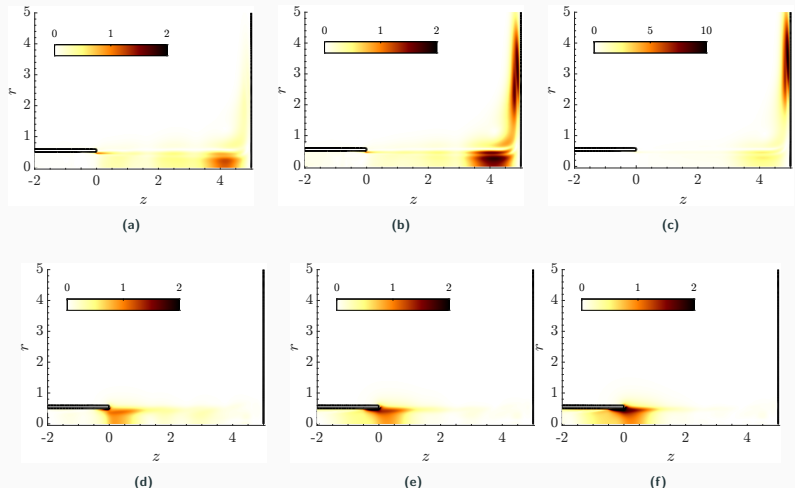
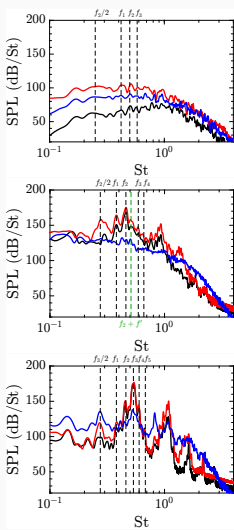


Figure 3: (a-c) Map $S_{u,s}^{(hyd,ac)}$ for $M_\infty = 0.6$, $M_\infty = 0.5$ and $M_\infty = 0.4$ for mode with $St \approx 0.5$. (e-f) Map $S_{u,s}^{(ac,hyd)}$ for the same modes.

Summary - Conclusions



1. Linear stability & Wave decomposition of the *linear global mode or main feedback mechanism.*
 - Existence of an arc of linear global modes for every Mach number. Thus, the feedback mechanism exists for every Mach number.
 - The wave decomposition confirms the theoretical predictions and supports the quantization of modes in an arc.
2. Transition from tonal to broadband noise
 - Resonant normal form accounts for the dynamics and mutual interactions between limit cycles of the arc. Departure from tonality due to: Imperfect quantization of the arc of modes.
 - The spatial location of the wavemaker of acoustic waves induced by the vortical component of the flow gradually changes when decreasing Mach. The wavemaker at low Mach is localized in a chaotic region, thus providing a less coherent closure of the feedback.